Histol Histopathol (2014) 29: 377-386
DOI: 10.14670/HH-29.377

http://www.hh.um.es

Histology and Histopathology
Cellular and Molecular Biology

Proteomic analysis in usual and nonspecific interstitial pneumonia

Ichiyo Ohara[1], Shinsuke Aida[2], Hideyuki Shimazaki[1], Hideo Kobayashi[3], Hitoshi Tsuda[4], Tosifusa Toda[5], Kuniaki Nakanishi[1] and Seiichi Tamai[1]

[1]Department of Laboratory Medicine, National Defense Medical College Hospital, Tokorozawa, [2]Department of Pathology, Mita Hospital, International University of Health and Welfare, Tokyo, Departments of [3]Respiratory Medicine and [4]Basic Pathology, National Defense Medical College, Tokorozawa and [5]Department of Gene Regulation and Protein Function, Tokyo Metropolitan Institute of Gerontology, Tokyo, Japan

Summary. Differentiating nonspecific interstitial pneumonia (NSIP) from usual interstitial pneumonia (UIP) is important for the determination of both treatment and prognosis. Using two-dimensional fluorescence difference gel electrophoresis (2D-DIGE), we examined 8 UIPs, 8 NSIPs, and 30 normal lung tissues. Comparisons with control in 2D-DIGE showed that (a) in UIP, nine protein spots were significantly upregulated and seven were significantly downregulated, (b) in NSIP, four protein spots were significantly upregulated and nine were significantly downregulated. The detected proteins were analyzed by MALDI-TOF mass spectrometry, allowing qualitative differences in vimentin subtypes to be characterized. One vimentin subtype was upregulated in UIP, while another one was downregulated in NSIP (vs. control). These different characteristics were partially supported by the results of Western blot analysis. Our immunohistochemistry revealed vimentin expression within fibroblasts (a) in fibroblastic foci in UIP and (b) in fibrotic alveolar walls in NSIP. Differences in vimentin subtypes may provide useful biomarkers for separating NSIP from UIP, alongside differences in histological characteristics.

Key words: Proteomics, Usual interstitial pneumonia, Nonspecific interstitial pneumonia, Two-dimensional fluorescence difference gel electrophoresis

Offprint requests to: Kuniaki Nakanishi MD, Department of Laboratory Medicine, National Defense Medical College Hospital, Tokorozawa 359-8513, Japan. e-mail: nknsknak@ndmc.ac.jp

Introduction

Idiopathic pulmonary fibrosis (IPF) is a progressive and usually fatal interstitial lung disease. In 1994, the clinicopathologic entity of nonspecific interstitial pneumonia (NSIP) was described among the idiopathic interstitial pneumonias (IIP) (Katzenstein and Fiorelli, 1994). Although NSIP is the closest mimic of usual interstitial pneumonia (UIP), the 5-year survival rate is 70-100% for NSIP, while the median survival in UIP is approximately 3 years (Katzenstein and Fiorelli, 1994; Bjoraker et al., 1998; Nagai et al., 1998; Daniil et al., 1999; Nicholson et al., 2000; Travis et al., 2000; Raghu et al., 2011). Further, patients with NSIP respond better to therapy (Katzenstein and Fiorelli, 1994; Bjoraker et al., 1998; Nagai et al., 1998; Daniil et al., 1999; Nicholson et al., 2000; Travis et al., 2000). Thus, it is important to differentiate NSIP from UIP for the purpose of determining both the required treatment and the prognosis in a given patient.

For the diagnosis of IIP, surgical lung biopsy, including video-assisted thoracoscopic surgery (VATS), is considered to be the "gold standard", but is a relatively invasive examination. About 10 years ago, this "gold standard" for differentiating between UIP and NSIP received a challenge from noninvasive radiologic imaging, such as high-resolution computed tomography (HRCT) (Johkoh et al., 1999; Hartman et al., 2000; Raghu et al., 2011). However, the ability of HRCT to distinguish NSIP from UIP is controversial because of the variety of radiological findings in NSIP (Johkoh et al., 1999; Hartman et al., 2000).

The proteomic approach has emerged as a powerful tool that can (a) provide protein-expression profiles, which may be useful both for predicting clinical events or therapeutic responses, and/or for unraveling disease mechanisms, and (b) allow analysis of the quantities of certain proteins present in different conditions (Toda and Kimura, 1997; Massion and Caprioli, 2006). Moreover, proteomic studies may well be a key propulsive force favoring the discovery of new biomarkers. Within the last few years, several studies have carried out proteomic analysis of lung tissue or bronchoalveolar lavage (BAL) fluid obtained from patients with parenchymal lung diseases, including IPF (Rottoli et al., 2005; Kinnula et al., 2009; Korfei et al., 2011; Okamoto et al., 2012). In the present study, we used proteomics analysis informed by two-dimensional fluorescence difference gel electrophoresis (2D-DIGE) to address the difference in protein conditions between UIP and NSIP. To that end, we examined 16 specimens from UIPs (8) and NSIPs (8), each with a fibrotic pattern, as well as 30 normal lung tissues.

Materials and methods

Patients and histopathologic diagnosis

We obtained 16 lung samples by VATS from patients with UIP (8 samples; 8 patients) and NSIP (8 samples; 8 patients) in the National Defense Medical Hospital from January 1996 to December 2006. Two independent experienced lung pathologists (SA and IO) diagnosed pathologic specimens obtained from these patients. Normal control lung samples were excised from surgically resected lung tissues obtained from 30 patients with lung cancer (non-smokers and with no known exposure to silica) from January 2005 to December 2007. All samples were immediately frozen in liquid nitrogen for proteome analysis. Written informed consent was obtained from all patients, and the protocols were approved by the institutional review board of the National Defense Medical College.

Protein extraction

A 15 mg portion of each lung sample was washed with normal saline and then homogenized on ice in 250 μl lysis buffer [8.3 M urea, 0.2% (w/v) sodium dodecyl sulfate (SDS), 2% (v/v) Triton X-100, 65 mM DL-dithiothreitol, 2% Pharmalyte (pH 3-10)], containing 10 μl protein inhibitor cocktail (Sigma Chemical Co., St Luis, MO). For this, we used a Sample Grinding Kit (GE Healthcare, Buckinghamshire, UK). After centrifugation (15,000 rpm for 5 min), the supernatant fluid was collected, and adjusted to pH 8.0-9.0 using 50 mM sodium hydroxide. Protein concentrations were determined using the DC Protein Assay system (Bio-Rad Laboratories, Hercules, CA). The protein concentration of each sample was adjusted to 5-10 mg/ml.

Two dimensional (2D) SDS-polyacrylamide gel electrophoresis

The 2D SDS-polyacrylamide gel electrophoresis (SDS-PAGE) protocol used here was adapted from Toda and Kimura (1997). Briefly, isoelectric focusing (IEF) was carried out using immobilized pH gradient (IPG) strips [18 cm, pH 4-7; Immobiline™ DryStrip (Amersham Bioscience, Uppsala, Sweden)]. Protein IEF was performed at 20°C using a CoolPhoreStar IPG-IEF (Anatech Co., Tokyo, Japan) as follows: step 1 at 500 volts (V) for 2 h, step 2 at 700 V for 1 h, step 3 at 1,000 V for 1 h, step 4 at 1,500 V for 1 h, step 5 at 2,000 V for 1 h, step 6 at 2,500 V for 1 h, step 7 at 3,000 V for 1 h, and step 8 at 3,500 V for 10 h. In this way, a total of 46,700 Volt-hours (Vh) was reached. Strips were washed for 30 min in an equilibration buffer [6 M urea, 32 mM DL-dithiothreitol, 0.025 M Tris-HCl pH 6.8, 2% (w/v) SDS, 0.005% (w/v) BPB, and 30% (v/v) glycerol], followed by washing for 20 min with a reduction buffer [0.025 M Tris-HCl pH 6.8, 2% (w/v) SDS, 0.005% (w/v) BPB, 30% (v/v) glycerol, and 0.25 M iodoacetamide]. SDS-PAGE, which was performed using 10% polyacrylamide gels (18x18 cm), was run at 25 mA for 5 h in a CoolPhoreStar SDS-PAGE Tetra-200 (Anatech Co.). The gels were washed overnight in fix solution [50% methanol (MeOH), 10% acetic acid], and stained either with a ProteoSilver Plus Silver Stain Kit (Sigma-Aldrich, St Louis, MO) or with SYPRO Ruby (Bio-Rad Laboratories), in accordance with the manufacturers' protocols. In a previous study, this technique identified about 590 silver-stained spots in the 2D-PAGE gel pattern of human diploid fibroblast protein, using IPG strips (pH 3.5-10) (Toda and Kimura, 1997).

Protein labeling

Equal amounts of proteins from 30 normal lung samples were pooled together as the internal standard, because the 2D SDS-PAGE gel images obtained from the 30 normal samples showed no significant differences. Proteins were minimally labeled according to the manufacturer's instructions (CyDye DIGE fluor minimal labeling kit; GE Healthcare). Briefly, each minimal CyDye was reconstituted in fresh N, N-dimethylformamide (DMF), and a 400 pmol quantity was used to label 50 μg of protein at pH 8.5. Cy2 was used to label the pooled internal standard. Cy3 and Cy5 were used for random labeling of NSIP, UIP, and normal control samples. The labeling reaction proceeded on ice in the dark for 30 min, until terminated by the addition of 1 μl 10 mM lysine (on ice in the dark for 10 min).

Two-dimensional fluorescence difference gel electrophoresis (2D-DIGE)

Following the labeling reaction, 160 μg of each of the Cy2-, Cy3-, and Cy5- labeled samples were mixed.

Samples were actively rehydrated into 18-cm pH 4-7 Immobiline DryStrips, and these were placed in a strip holder and then focused at 20°C, using a CoolPhoreStar IPG-IEF as described above. The strips were rehydrated in an equilibration buffer, and then proteins were further separated on 10% SDS-PAGE gels casted upon low-fluorescence glass plates, utilizing a CoolPhoreStar SDS-PAGE Tetra-200.

Scanning and image analysis

After 2D-DIGE, the gels were scanned using an Ettan DIGE imager (GE Amersham) at 100 μm resolution, as elaborated in the equipment setup instructions. The Cy2-, Cy3-, and Cy5-labeled images for each gel were scanned at excitation/emission wavelengths of 488/520 nm, 540/595 nm, and 635/680 nm, respectively. After scanning the fluorophores in each gel (mean, 6-8 times for each specimen), the images were imported into ImageMaster 2D Platinum (GE Amersham) for spot detection, according to the manufacturer's recommendations. After spot detection, the abundance differences were expressed as the normalized volume ratio (Cy3:Cy2 or Cy5:Cy2). When the spot-volume ratio obtained for the UIP or NSIP sample over the control sample was more than 1.6 or more negative than -1.6, and p was <0.05 by an independent Student's t-test, those protein spots were marked.

Protein digestion, mass spectrometry, and protein identification

Spots in the maps for which the intensity differed significantly between either UIP or NSIP and the control sample were selected for identification by mass spectrometry. Spots were excised with a 1.8 mm core from the SYPRO Ruby-stained gel using FluoroPhoreStar 3000 (Anatech Co.) for digestion. Spots were washed in reduction buffer (0.1 ml of 1.5 mg/ml dithiothreitol in 100 mM ammonium bicarbonate) for 30 min, alkalized in 0.1 ml of 10 mg/ml iodoacetamide in 100 mM ammonium bicarbonate for 30 min, destained (in 100 mM ammonium bicarbonate in 50% MeOH for 15 min twice and in 100 mM ammonium bicarbonate in 50% acetonitrile for 10 min three times), and finally incubated in 0.1 ml of 100% acetonitrile for 5 min. Gels were then dried completely by vacuum-drying. In-gel digestion was performed at 37°C overnight using 20 μg/ml sequencing grade trypsin (Promega) in 40 mM ammonium bicarbonate. To achieve complete peptide recovery, sequential extraction steps [10% trifluoroacetic acid (TFA), 50% acetonitrile at room temperature for 20 min] were carried out three times using the digested samples. The supernatants containing peptides were collected, and then concentrated and dried. Peptides were mixed with equal amounts of matrix solution [α-cyano-4-hydroxy-cinnamic acid (CHCA) in 0.05% TFA, 50% acetonitrile], immediately loaded onto the target plate, and allowed to air-dry at room temperature. MALDI-TOF mass spectrometry was performed using an AXIMA-CFR Plus (Shimadzu Co., Kyoto, Japan) according to the manufacturer's instructions. Protein identification was carried out by Peptide Mass Fingerprinting (PMF) analysis with the aid of Mascot software, comparisons being made with the NCBInr (National Center for Biotechnology Information non-redundant) sequence databases.

Western blotting analysis

After 2D SDS-PAGE (using the same samples as those used for 2D-DIGE), proteins were transferred to polyvinylidene difluoride membranes (PVDF, Hybond-N+; Amersham Biosciences, Piscataway, NJ). The membranes were blocked with 5% fat-free dry milk (Block Ace; Dainippon Pharmaceutical, Osaka, Japan) in Tris-buffered saline (0.025 M Tris-HCl, pH 7.4) containing 0.1% Tween 20 (TBST) for 1 h at room temperature, and incubated overnight with monoclonal mouse vimentin antibody (clone: V9; DAKO Cytomation, Glostrup, Denmark) diluted at 1:500 in TBST with 1% bovine serum albumin. After being washed with TBST three times, the membranes were further incubated for 1 h at room temperature with the corresponding horseradish peroxidase-conjugated secondary antibody (DAKO Cytomation) diluted at 1:3,000 in TBST with 1% bovine serum albumin, and then washed with TBST three times. The immunoreactive protein spots were visualized by means of an Enhanced Chemiluminescence ECL™ kit (Amersham Biosciences) using a LAS 3,000 system (Fuji Photo Film, Tokyo, Japan).

Immunohistochemistry

We applied the polymer-peroxidase method (EnVision+/HRP; Dako Cytomation, Denmark) to deparaffinized sections of 8 NSIPs and 8 UIPs using the monoclonal mouse vimentin antibody (DAKO Cytomation) diluted at 1:100. The antigen-retrieval condition was autoclaving in Target retrieval solution high pH (DAKO Cytomation) for 15 min.

Data analysis

Statistical analysis of the difference between two groups was performed using an independent Student's t-test. A p value of less than 0.05 was considered significant.

Results

Clinical and histological characteristics of UIP and NSIP patients

Two pathologists (SA and IO) diagnosed 8 patients with histological UIP and 8 patients with histological

fibrotic NSIP. Compared with the NSIP patients, UIP patients were more likely to be men, and to have greater elevations of serum KL-6 ($p<0.0001$) and serum surfactant protein D ($p=0.0014$). In UIP patients, the histological characteristics were a patchy geographical distribution and heterogeneity in terms of the stage of pathology in different regions (such as patchy lung involvement with frequent subpleural, paraseptal, and/or peribronchiolar distribution), dense fibrosis causing remodeling of the lung architecture with frequent "honeycomb" fibrosis, and fibroblastic foci scattered at the edges of the dense scars. Histological fibrotic NSIP patients were characterized by dense or loose interstitial fibrosis lacking the temporal heterogeneity and/or patchy features of UIP, and by the preservation of the lung architecture (Table 1).

Identification of differentially expressed proteins by 2D SDS-DIGE

The 2D-PAGE gel images obtained from the samples of 30 normal lung tissues were not significantly different from each other, particularly within the IEF range pH 4.5 to pH 6.5 and molecular weight range 15,000 to 200,000 kDa (Fig. 1). Therefore, equal amounts of proteins from the 30 normal lung samples were used to provide the average normal lung samples. The 2D SDS-DIGE process was carried out 6-8 times for each of the 2 groups (viz. each sample in the UIP group and average normal lung, and each sample in the NSIP group and average normal lung).

In 2D SDS-DIGE, a total of about 365 protein spots was matched between UIP and average normal lung (Fig. 2a). When the spot-volume ratio obtained for the UIP sample over the average normal lung sample was considered to indicate a significant "UIP vs. normal" difference (i.e., if the ratio was more than 1.6 or more negative than -1.6), nine protein-spot features were found to be significantly upregulated in UIP, whereas seven protein-spot features were found to be significantly downregulated in UIP. Finally, three of the upregulated proteins (nos. 1, 4, and 5) and two of the downregulated proteins (nos. 12 and 16) were identified by MALDI-TOF mass spectrometry, because the remaining six upregulated proteins and five

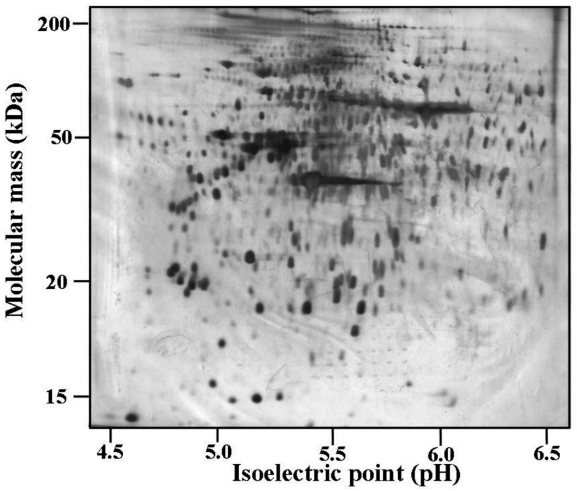

Fig. 1. Two-dimensional sodium dodecyl sulfate (SDS)-polyacrylamide gel electrophoresis (2D SDS-PAGE) of average normal lung tissues obtained from 30 patients with lung cancer. Proteins were extracted and separated at pH 4-7 in 18-cm immobilized pH gradient (IPG) strips for the first dimension and in 10% polyacrylamide gel for the second dimension. The gels were stained with silver.

Table 1. Clinicopathological findings in usual interstitial pneumonia (UIP) and nonspecific interstitial pneumonia (NSIP).

	UIP (n=8)	NSIP (n=8)	p value**
Age (yrs)	65.4±6.7*	63.6±8.8	0.65
Sex			
Male	7	4	
Female	1	4	
Erythrocyte sedimentation rate (1hr) (normal range: 1-7 for male, 3-11 for female)	27.4±8.8	22.6±10.6	0.34
Serum			
Lactate dehydrogenase (IU/L) (normal range: 100-225)	197±33	213±28	0.31
KL-6 (U/ml) (normal range: <500)	1290±97	887±107	<0.0001
Surfactant protein D (ng/ml) (normal range: <110)	241±35	155±49	0.0014
Pathological findings			
Patchy lung involvement	8	0	
Frequent subpleural, paraseptal and/or peribronchiolar distribution	8	1	
Dense fibrosis causing remodeling of lung architecture with frequent "honeycomb" fibrosis	8	4	
Fibroblastic foci scattered at the edges of the dense scars	8	1	
Interstitial inflammation, mild to moderate	8	8	
Dense or loose interstitial fibrosis lacking the temporal heterogeneity and/or patchy features of UIP	0	8	
Lung architecture is often preserved	0	8	

*: mean ± standard deviation; **: Statistical analysis of the difference between two groups was performed using an independent Student's t-test.

downregulated proteins could not be determined (Fig. 3a). Of the five corresponding proteins, the three upregulated proteins were identified as a subtype of "vimentin" (no. 1), a subtype of "haptoglobin protein" (no. 4), and "chain A, crystal structure of the Ga module complex with human serum albumin" (no. 5), while the two downregulated proteins were a subtype of "annexin VI isoform 1" (no. 12) and "chain A, human heart L-lactate dehydrogenase H chain, ternary complex with NADH and oxamate" (no. 16) (Tables 2, 3).

Similarly, between NSIP and average normal lung a total of about 288 protein spots was matched (Fig. 2b). Using the same criteria as above, in NSIP four protein-spot features were found to be significantly upregulated and nine protein-spot features to be significantly downregulated (Fig. 3b). Although one of these upregulated proteins and two of the downregulated proteins could not be determined, the remaining nine corresponding proteins, comprising three upregulated proteins (nos. 5, 17, and 18) and seven downregulated proteins (nos. 12, 16, 19, 20, 23, 24, and 25), could be identified. The three upregulated proteins were a subtype of "chain A, crystal structure of the Ga module complex with human serum albumin" (no. 5), a subtype of "haptoglobin protein" (no. 17), and "L-plastin" (no. 18), while the seven downregulated proteins were a subtype

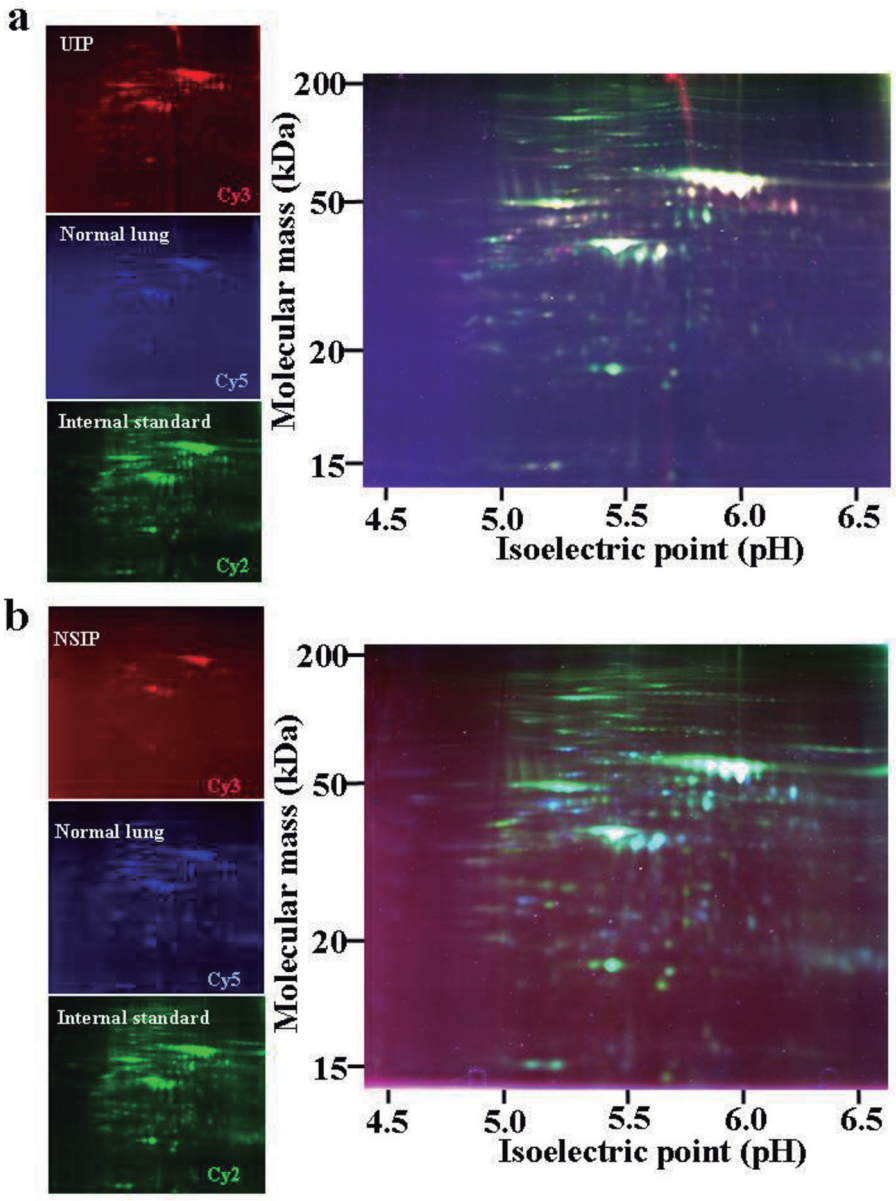

Fig 2 Two-dimensional fluorescence difference gel electrophoresis (2D-DIGE) pictures of overlays of three-dye scans in usual interstitial pneumonia (UIP) and normal lung **(a)** or nonspecific interstitial pneumonia (NSIP) and normal lung **(b)**. Proteins were extracted and separated at pH 4-7 in 18-cm immobilized pH gradient (IPG) strips for the first dimension and in 10% polyacrylamide gel for the second dimension. Images were acquired using a Typhoon 9400 scanner. Dots represent spots detected by the ImageMaster 2D Platinum. Cy2 (green) image of proteins was obtained from an internal standard in the pool of all samples, Cy5 (blue) image of proteins was from normal lung, and Cy3 (red) images of proteins were from UIP **(a)** or NSIP **(b)**.

of "annexin VI isoform 1" (no. 12), "chain A, human heart L-lactate dehydrogenase H chain, ternary complex with NADH and oxamate" (no. 16), two subtypes of "ACTB protein" (nos. 19 and 23), a subtype of "vimentin" (no. 20), and two subtypes of "chain A, crystal structure of lipid-free human apolipoprotein A-1" (nos. 24 and 25) (Tables 4, 5).

Protein validation by Western blot analysis and immunohistochemistry

Among the proteins in UIP or NSIP that could be

Table 2. Proteins upregulated in usual interstitial pneumonia (UIP) [vs. normal lung tissue (N)], as identified by MALDI-TOF MS.

Spot No.	Protein name	Accession No.	MW	pI	Protein score	Sequence coverage (%)
1	Vimentin	gil62414289	53676	5.06	312	70
4	Haptoglobin protein	gil47124562	31647	8.48	104	33
5	Chain A, crystal structure of the Ga module complex with human serum albumin	gil55669910	67174	5.57	278	52

Table 3. Proteins downregulated in usual interstitial pneumonia (UIP) [vs. normal lung tissue (N)], as identified by MALDI-TOF MS.

Spot No.	Protein name	Accession No.	MW	pI	Protein score	Sequence coverage (%)
12	Annexin VI isoform 1	gil71773329	76168	5.42	360	56
16	Chain A, human heart L-lactate dehydrogenase H chain, ternary complex with NADH and oxamate	gil13786847	36769	5.72	218	58

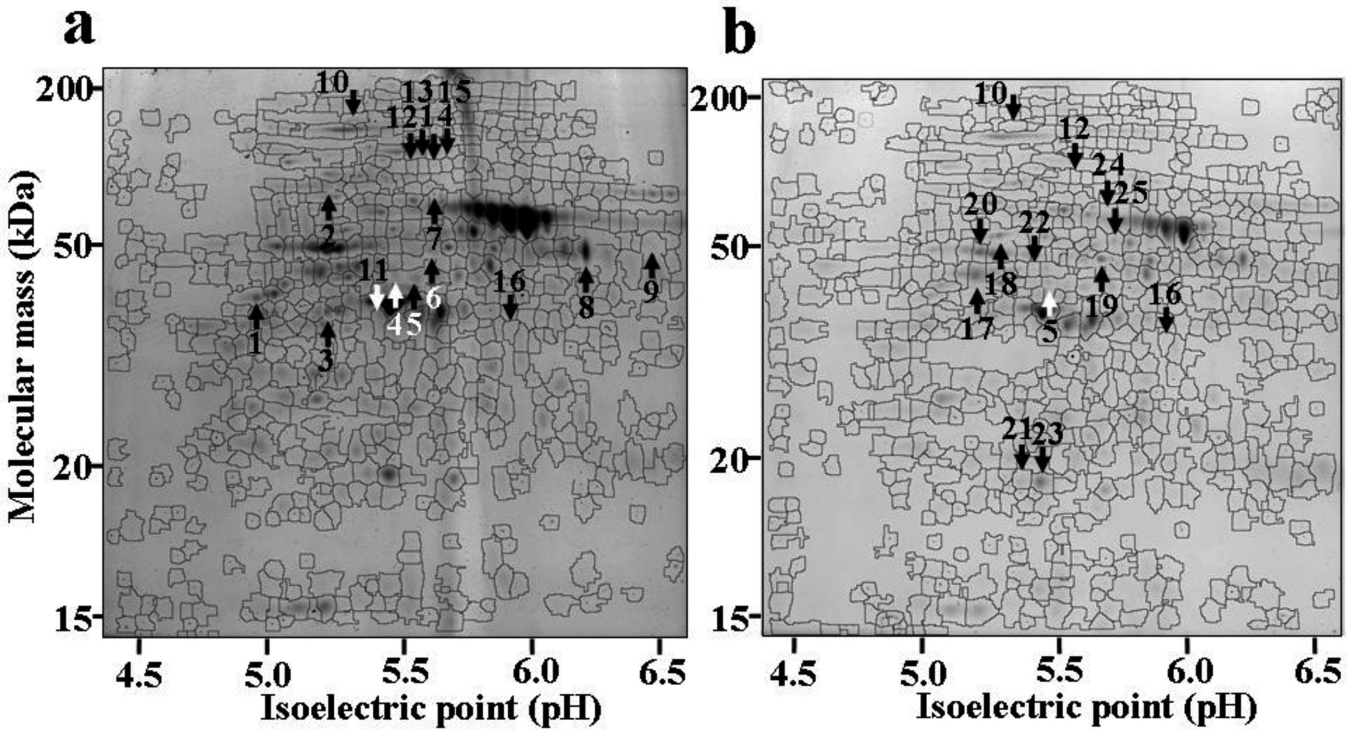

Fig. 3. Protein spots in a representative two-dimensional fluorescence difference gel electrophoresis (2D-DIGE) picture that were significantly different between usual interstitial pneumonia (UIP) and normal lung **(a)**, or between nonspecific interstitial pneumonia (NSIP) and normal lung **(b)**. Circles surrounded by lines represent spots detected by the ImageMaster 2D Platinum. (a) Nine protein spots were found to be significantly upregulated in UIP (> 1.6 average ratio, $p<0.05$). Seven protein spots were significantly downregulated in UIP (average ratio more negative than -1.6 average ratio, $p<0.05$). (b) Four protein spots were found to be significantly upregulated in NSIP (> 1.6 average ratio, $p<0.05$). Seven protein spots were significantly downregulated in NSIP (< -1.6 average ratio, $p<0.05$).

differentiated from those in the normal lung using 2D SDS-DIGE and MALDI-TOF mass spectrometry, three proteins were identified as vimentin, haptoglobin protein, and annexin VI isoform 1. Among these, qualitative differences in vimentin subtypes were characterized, particularly an upregulated subtype (spot no. 1) in UIP and a downregulated subtype (spot no. 20) in NSIP. To evaluate vimentin expressions in UIP and NSIP, we examined 2D SDS-PAGE gels using Western blotting analysis. This analysis revealed expressions of at least 8 vimentin subtypes [spot nos. 1 and 20, and 6 other spots (α, ß, γ, δ, ε and ζ)] on 2D SDS-PAGE gel in UIP and at least 7 vimentin subtypes [spot nos. 1 and 20, and 5 other spots (α, γ, δ, ε and ζ)] on 2D SDS-PAGE gel in NSIP (Fig. 4). When UIP was compared with NSIP, the expression of spot no. 1 was stronger in UIP than in NSIP. The expression of spot no. 20 in UIP was similar to that in NSIP. Spots α and ß were expressed in UIP, but not in NSIP. The expressions of spots γ, δ and ε in UIP appeared to be strong, while that of spot ζ in UIP appeared to be weak (in each case, versus NSIP). However, we could not analyze the degrees of spot

Table 4. Proteins upregulated in nonspecific interstitial pneumonia (NSIP) [vs. normal lung tissue (N)], as identified by MALDI-TOF MS.

Spot No.	Protein name	Accession No.	MW	pI	Protein score	Sequence coverage (%)
5	Chain A, crystal structure of the Ga module complex with human serum albumin	gil55669910	67174	5.57	145	47
17	Haptoglobin protein	gil47124562	31647	8.48	105	41
18	L-plastin	gil4504965	70815	5.20	153	38

Table 5. Proteins downregulated in nonspecific interstitial pneumonia (NSIP) [vs. normal lung tissue (N)], as identified by MALDI-TOF MS.

Spot No.	Protein name	Accession No.	MW	pI	Protein score	Sequence coverage (%)
12	Annexin VI Isoform 1	gil 71773329	76168	5.42	360	56
16	Chain A, human heart L-lactate dehydrogenase H chain, ternary complex with NADH and oxamate	gil13786847	36769	5.72	218	58
19	ACTB protein	gil15277503	40536	5.55	81	26
20	Vimentin	gil 57471646	49680	5.19	81	56
23	ACTB protein	gil15277503	40536	5.55	72	25
24	Chain A, crystal structure of lipid-free human apolipoprotein A-1	gil90108664	28061	5.27	261	81
25	Chain A, crystal structure of lipid-free human apolipoprotein A-1	gil90108664	28062	5.27	78	45

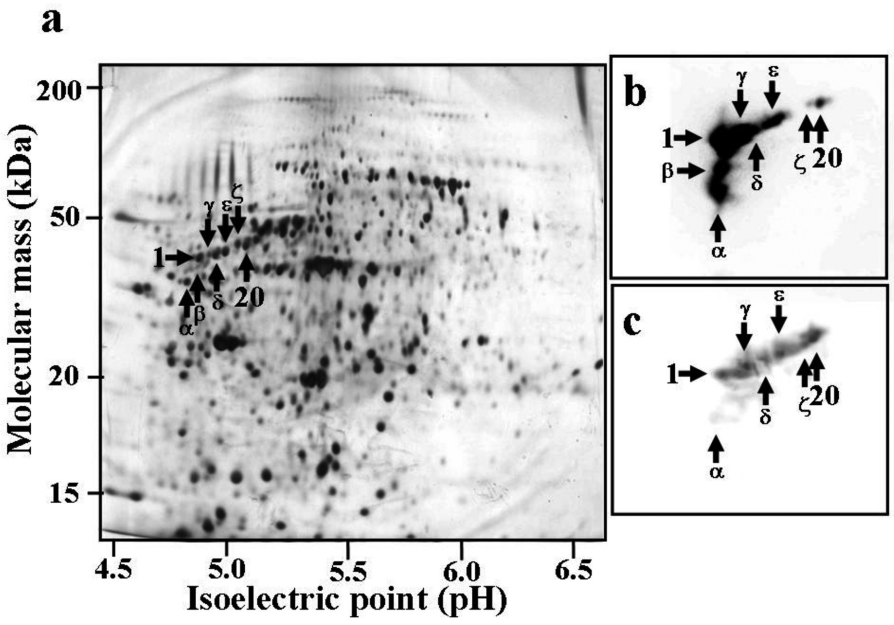

Fig. 4. Western blotting analysis for vimentin in two-dimensional sodium dodecyl sulfate (SDS)-polyacrylamide gel electrophoresis (2D SDS-PAGE) in usual interstitial pneumonia (UIP) **(b)** and nonspecific interstitial pneumonia (NSIP) **(c). a.** 2D SDS-PAGE of average normal lung tissues stained with silver. Western blotting analysis revealed expressions of at least 8 vimentin subtypes [spot nos. 1 and 20, and 6 other spots (α, ß, γ, δ, ε, and ζ)] in UIP **(b)** and at least 7 vimentin subtypes [spot nos. 1 and 20, and 5 other spots (α,γ, δ, ε, and ζ))] in NSIP **(c)**. When UIP was compared with NSIP, the expression of spot no. 1 was stronger in UIP than in NSIP. The expression of spot no. 20 in UIP was similar to that in NSIP. Spots α and ß were expressed in UIP, but not in NSIP. The expressions of spots γ, δ, and ε in UIP appeared to be strong, and that of spot ˙ in UIP appeared to be weak, compared with their expressions in NSIP.

expression because a marker protein was not applied in 2D SDS-PAGE. The result obtained for spot no. 1 using Western blotting analysis appeared consistent with the expression differences revealed by 2D SDS-DIGE.

By immunohistochemistry, vimentin was detected within both the endothelial cells and smooth muscle cells of blood vessels, within fibroblasts in the fibrotic alveolar walls, and within alveolar macrophages in both UIP and NSIP, but not within either alveolar epithelial cells or ciliated columnar epithelial cells in the bronchioles (Fig. 5). Fibroblasts within fibroblastic foci expressed vimentin strongly in UIP, while fibroblasts in the fibrotic alveolar walls expressed it in NSIP.

Discussion

As tools for distinguishing NSIP from UIP, noninvasive imaging equipment and analysis of BAL

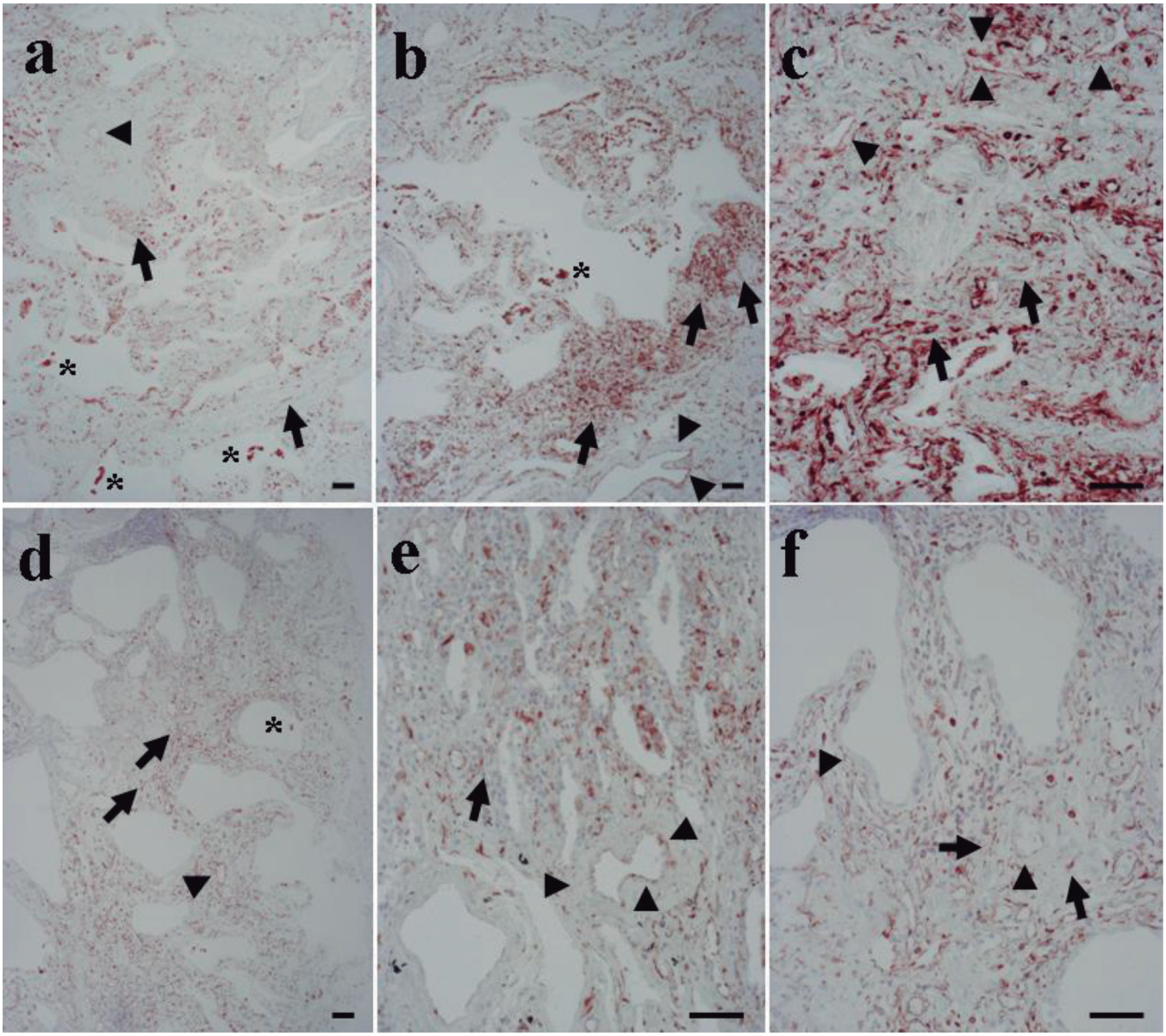

Fig. 5. Immunohistochemistry for vimentin in usual interstitial pneumonia (UIP) and nonspecific interstitial pneumonia (NSIP). In slides of UIP **(a, b, c),** vimentin expression can be seen within fibroblasts (arrows) in fibroblastic foci, as well as within endothelial cells (arrowheads) in blood vessels and within macrophages (asterisks) in the alveolar spaces. In slides of NSIP **(d, e, f),** vimentin expression can be seen within fibroblasts (arrows) in the alveolar walls, as well as within endothelial cells (arrowheads) in blood vessels and within macrophages (asterisks) in the alveolar spaces. Bars: 100 μm.

fluid have been challenged on the grounds of inconsistent findings (Johkoh et al., 1999; Hartman et al., 2000; Wattiez, 2000; Okamoto et al., 2012), and only a few novel radiological imaging techniques and biomarkers have been established for differential diagnosis. In the present study, we examined 8 UIP, 8 NSIP with a fibrotic pattern, and 30 normal lung tissues using proteomics analysis informed by 2D-DIGE, and we found evidence suggesting that qualitative differences in vimentin subtypes may characterize the distinction between UIP and NSIP. These distinctive characteristics were supported partially by Western blotting analysis, although in our immunohistochemistry vimentin was expressed both within fibroblasts in fibroblastic foci in UIP and within fibroblasts of fibrotic alveolar tissue in NSIP. On the basis of these findings, differences in vimentin subtypes may provide useful biomarkers for separating NSIP from UIP, alongside the histological characteristics.

Whether we compared NSIP or UIP with average normal lung using 2D-DIGE, a subtype of haptoglobin protein was found to be upregulated (spot no. 4 in UIP and spot no. 17 in NSIP), while a subtype of annexin VI isoform 1 was downregulated (spot no. 12 in both UIP and NSIP). Haptoglobin protein is one of the acute-phase proteins, and plays an important inhibitory role in inflammation (McPherson, 2007). Its biosynthesis occurs not only in liver, but also in lung. Moreover, in a recent study of chronic hypersensitivity pneumonia, application of 2D-PAGE (pH 3 to 7) revealed that in BAL fluid, haptoglobin ß was higher in the histologic UIP pattern than in the histologic NSIP pattern (Okamoto et al., 2012). Therefore, we suggest that inflammation of the alveolar walls may be a continuing process during the course of fibrosis formation in UIP and NSIP. However, we speculate that different subtypes of haptoglobin protein may be associated with the pathogenesis of different types of fibrosis between these diseases, although we could not investigate this possibility. Annexin VI, a member of the Ca^{2+}-dependent phospholipid-binding proteins, is expressed in many tissues. In cardiac fibrosis, it is expressed immunohistochemically in the interstitial tissue, suggesting a role in fibrosis development (Trouve' et al., 1999). Those results are in contrast to our data. Although the reason for this discrepancy is not clear, factors such as a difference in the isoform involved in the development of cardiac fibrosis vs. lung fibrosis and/or different actions against different target organs may be suggested. Interestingly, a recent study using proteomic analysis reported 3 downregulated proteins of the annexin family (annexins A1, A2, and A3) in UIP lung tissues compared with normal tissues (Korfei et al., 2011).

In the present study, 2D-DIGE demonstrated qualitative differences in vimentin subtypes between NSIP and UIP, but inspection of the immunohistochemical staining pattern revealed no such differences. Likewise, Korfei et al. (2011) reported upregulation of a vimentin subtype (similar in both molecular weight and isoelectric point to the vimentin in our results) in UIP lung tissues compared with control lung tissues, although they did not perform Western blotting analysis. It is known that vimentin is present within mesenchymal cells (e.g., fibroblasts). Studies performed about 10 years ago found that the serum level of anti-vimentin antibody was elevated in patients with NSIP or UIP (versus that seen in volunteer control), and that it was significantly higher in patients with NSIP than in those with UIP (Yang et al., 2002; Fujita et al., 2003). In the latter study, the antigens toward this antibody were thought to be not only a vimentin protein of molecular weight 58,000, but also vimentin fragments produced by the actions of enzymes such as caspase (Fujita et al., 2003). Those authors suggested that vimentin and/or vimentin fragments might be associated with the development of IPF. In previous immunohistochemical studies, fibroblasts located within fibroblastic foci in UIP were shown to express vimentin and α-smooth muscle actin, suggesting an intermediate cell-type between fibroblasts and smooth muscle cells (Kuhn et al., 1989; Kuhn and McDonald, 1991; Walker et al., 2001). Furthermore, the fibroblastic foci were thought to be an indication of active ongoing fibrosis, and the fibroblasts detected within the fibroblastic foci were described as being of an activated myofibroblast phenotype (Kuhn et al., 1989; Walker et al., 2001). In experimental pulmonary fibrosis, an epithelial-to-mesenchymal transition (EMT) has been reported to occur in the lung during fibrogenesis, and such EMT cells have been shown by immunohistochemistry to express vimentin (Willis et al., 2005; Kim et al., 2006). On the basis of the present study and those cited above, qualitative differences in vimentin subtypes may be a useful marker for the separation of NSIP from UIP.

The present study had several limitations. First, we studied a small number of patients, so the significance of the reported statistical differences between UIP and NSIP may be low. Second, we could not identify every protein detected in this study. In our study, six upregulated proteins and five downregulated proteins in UIP (versus the average normal lung) and one upregulated protein and two downregulated proteins in NSIP (versus the average normal lung) could not be identified by MALDI-TOF mass spectrometry, for reasons that we could not determine. Furthermore, we could not confirm the identities of all the proteins that differed between UIP and NSIP using Western blotting analysis because of a lack of specific antibodies.

In conclusion, we have demonstrated, using proteomics analysis informed by 2D-DIGE, that qualitative differences in vimentin subtypes exist between UIP and NSIP. Although our data suggest that these qualitative differences may be useful biomarkers for the differentiation of NSIP from UIP, further studies, on a larger scale, will be needed to confirm or deny this idea.

Conflict of interest. The authors declare that they have no conflict of interest.

References

Bjoraker J.A., Ryu J.H., Edwin M.K., Myers J.L., Tazelaar H.D., Schroeder D.R. and Offord K.P. (1998). Prognostic significance of histopathologic subsets in idiopathic pulmonary fibrosis. Am. J. Respir. Crit. Care Med. 157, 199-203.

Daniil Z.D., Gilchrist F.C., Nicholson A.G., Hansell D.M, Harris J., Colby T.V. and duBois R.M. (1999). A histologic pattern of nonspecific interstitial pneumonia is associated with a better prognosis than usual interstitial pneumonia in patients with cryptogenic fibrosing alveolitis. Am. J. Respir. Crit. Care Med. 160, 899-905.

Fujita J., Bandoh S., Yang Y., Wu F., Ohtsuki Y., Yoshinouchi T. and Ishida T. (2003). High molecular weight vimentin complex is formed after proteolytic digestion of vimentin by caspase-3: detection by sera of patients with interstitial pneumonia. Microbiol. Immunol. 47, 447-451.

Hartman T.E., Swensen S.J., Hansell D.M., Colby T.V., Myers J.L., Tazelaar H.D., Nicholson A.G., Wells A.U., Ryu J.H., Midthun D.E., du Bois R.M. and Müller N.L. (2000). Nonspecific interstitial pneumonia: Variable appearance at high-resolution chest CT. Radiology 217, 701-705.

Johkoh T., Müller N.L., Cartier Y., Kavanagh P.V., Hartman T.E., Akira M., Ichikado K., Ando M. and Nakamura H. (1999). Idiopathic interstitial pneumonias: diagnostic accuracy of thin-section CT in 129 patients. Radiology 211, 555-560.

Katzenstein A.L. and Fiorelli R.F. (1994). Nonspecific interstitial pneumonia/fibrosis. Histologic features and clinical significance. Am. J. Surg. Pathol. 18, 136-147.

Kim K.K., Kugler M.C., Wolters P.J., Robillard L., Galvez M.G., Brumwell A.N., Sheppard D. and Chapman H.A. (2006). Alveolar epithelial cell mesenchymal transition develops in vivo during pulmonary fibrosis and is regulated by the extracellular matrix. Proc. Nalt. Acad. Sci. USA 103, 13180-13185.

Kinnula V.L., Ishikawa N., Bergmann U. and Ohlmeier S. (2009). Proteomic approaches for studying human parenchymal lung diseases. Expert. Rev. Proteomics 6, 619-629.

Korfei M., Schmitt S., Ruppert C., Henneke I., Markart P., Loeh B., Mahavadi P., Wygrecka M., Klepetko W., Fink L., Bonniaud P., Preissner K.T., Lochnit G., Schaefer L., Seeger W. and Guenther A. (2011). Comparative proteomic analysis of lung tissue from patients with idiopathic pulmonary fibrosis (IPF) and lung transplant donor lungs. J. Proteome Res. 10, 2185-2205.

Kuhn C. 3rd., Boldt J., King T.E. Jr, Crouch E., Vartio T. and McDonald J.A. (1989). An immunohistochemical study of architectural remodeling and connective tissue synthesis in pulmonary fibrosis. Am. Rev. Respir. Dis. 140, 1693-1703.

Kuhn C. and McDonald J.A. (1991). The roles of the myofibroblasts in idiopathic pulmonary fibrosis. Ultrastructural and immunohistochemical features of sites of active extracellular matrix synthesis. Am. J. Pathol. 138, 1257-1265.

Massion P.P. and Caprioli R.M. (2006). Proteomic strategies for the characterization and the early detection of lung cancer. J. Thorac. Oncol. 1, 1027-1039.

McPherson R.A. (2007). Specific proteins. In: Henry's clinical diagnosis and management by laboratory methods. McPherson R.A. and Pincus M.R. (eds). 21st edition. Saunders Elsevier. Philadelphia. pp 237-238.

Nagai S., Kitaichi M., Itoh H., Nishimura K., Izumi T. and Colby T.V. (1998). Idiopathic nonspecific interstitial pneumonia/fibrosis: comparison with idiopathic pulmonary fibrosis and BOOP. Eur. Respir. J. 12, 1010-1019.

Nicholson A.G., Colby T.V., DuBois R.M., Hansell D.M. and Wells A.U. (2000). The prognostic significance of the histologic pattern of interstitial pneumonia in patients presenting with the clinical entity of cryptogenic fibrosing alveolitis. Am. J. Respir. Crit. Care Med. 162, 2213-2217.

Okamoto T., Miyazaki Y., Shirahama R., Tamaoka M. and Inase N. (2012). Proteome analysis of bronchoalveolar lavage fluid in chronic hypersensitivity pneumonitis. Allergol. Int. 61, 83-92.

Raghu G., Collard H.R., Egan J.J., Martinez F.J., Behr J., Brown K.K., Colby T.V., Cordier J.F., Flaherty K.R., Lasky J.A., Lynch D.A., Ryu J.H., Swigris J.J., Wells A.U., Ancochea J., Bouros D., Carvalho C., Costabel U., Ebina M., Hansell D.M., Johkoh T., Kim D.S., King T.E. Jr, Kondoh Y., Myers J., Muller N.L., Nicholson A.G., Richeldi L., Selman M., Dudden R.F., Griss B.S., Protzko S.L., Schunemann H.J., and ATS/ERS/JRS/ALAT Committee on Idiopathic Pulmonary Fibrosis. (2011). An official ATS/ERS/JRS/ALAT statement: idiopathic pulmonary fibrosis: evidence-based guidelines for diagnosis and management. Am. J. Respir. Crit. Care Med. 183, 788-824.

Rottoli P., Magi B., Perari M.G., Liberatori S., Nikiforakis N., Bargagli E., Cianti R., Bini L. and Pallini V. (2005). Cytokine profile and proteome analysis in bronchoalveolar lavage of patients with sarcoidosis, pulmonary fibrosis associated with systemic sclerosis and idiopathic pulmonary fibrosis. Proteomics 5, 1423-1430.

Toda T. and Kimura N. (1997). Standardization of protocol for immobiline 2-D PAGE and construction of 2-D PAGE protein database on World Wide Web home page. Jpn. J. Electrophoresis 41, 13-20.

Travis W.D., Matsui K., Moss J. and Ferrans V.J. (2000). Idiopathic nonspecific interstitial pneumonia: prognostic significance of cellular and fibrosing patterns: survival comparison with usual interstitial pneumonia and desquamative interstitial pneumonia. Am. J. Surg. Pathol. 24, 19-33.?

Trouve´ P., Legot S., Be´likova I., Marotte F., Be´ne´volensky D., Russo-Marie F., Samuel J.L. and Charlemagne D. (1999). Localization and quantitation of cardiac annexins II, V, and VI in hypertensive guinea pigs. Am. J. Physiol. 276 (Heart Circ. Physiol. 45), H1159–H1166.

Walker G.A., Guerrero I.A. and Leinwand L.A. (2001). Myofibroblasts: molecular crossdressers. Curr. Top Dev. Biol. 51, 91-107.

Wattiez R., Hermans C., Cruyt C., Bernard A. and Falmagne P. (2000). Human bronchoalveolar lavage fluid protein two-dimensional database: study of interstitial lung diseases. Electrophoresis 21, 2703-2712.

Willis B.C., Liebler J.M., Luby-Phelps K., Nicholson A.G., Crandall E.D., du Bois R.M. and Borok Z. (2005). Induction of epithelial-mesenchymal transition in alveolar epithelial cells by transforming growth factor-beta l: potential role in idiopathic pulmonary fibrosis. Am. J. Pathol. 166, 1321-1332.

Yang Y., Fujita J., Bandoh S., Ohtsuki Y., Yamadori I., Yoshinouchi T. and Ishida T. (2002). Detection of antivimentin antibody in sera of patients with idiopathic pulmonary fibrosis and non-specific interstitial pneumonia. Clin. Exp. Immunol. 128, 169-177.

Accepted September 10, 2013